International Multidisciplinary Research Journal Reviews (IMRJR)

International Multidisciplinary Research Journal Reviews (IMRJR)
A Peer-reviewed journal
Volume 1, Issue 4, December 2024
DOI 10.17148/IMRJR.2024.010405

Ni-Doping Effects on the Optical, Structural, Morphological, and Compositional Behavior of Sol-Gel Synthesized CuS Thin Films for Enhanced Optoelectronic Performance

Ikechukwu Ernest NWANKWO[1,2*], Ifeyinwa Euphemia OTTIH[1],

Emmanuel Onyebuchi ONYEBUEKE[1] and Chukwuemeka Innocent ELEKALACHI[1]

Department of Industrial Physics, Faculty of Physical Science, Chukwuemeka Odumegwu Ojukwu University Uli, Anambra State, Nigeria[1]

Department of Science Laboratory Technology, Federal Polytechnic Oko, Anambra State, Nigeria[2]

Abstract: Nickel-doped copper sulfide (Ni:CuS) thin films with varying thicknesses and morphologies were successfully synthesized on microscopic glass substrates via a sol-gel dip-coating method to investigate their potential for device applications. The primary precursors included copper (II) tetraoxosulphate (VI), sodium disulphide, and nickel (II) chloride hexahydrate as sources of Cu^{2+}, S^{2-}, and Ni^{2+} ions, respectively, with ethylene glycol serving as a stabilizing agent. The Ni:CuS thin films underwent optical, structural, morphological, and compositional characterizations using UV-Vis spectroscopy, X-ray diffraction (XRD), scanning electron microscopy (SEM), and energy-dispersive spectroscopy (EDS). Optical analysis revealed that the Ni:CuS films exhibited high absorbance values in the UV and NIR regions, while their refractive index increased significantly in the VIS-NIR regions. The bandgap energy decreased with increasing Ni concentration, with values of 2.66 eV, 2.50 eV, 2.41 eV, and 2.33 eV for films doped with 0.04 M, 0.06 M, 0.08 M, and 0.10 M Ni ions, respectively. XRD results confirmed the crystalline nature of the films with a hexagonal structure, while crystallite sizes for films doped with 0.02 M, 0.06 M, and 0.10 M Ni ions were determined as 19.45 nm, 19.54 nm, and 19.92 nm, respectively. EDS analysis confirmed the presence of Cu, Ni, and S, alongside trace elements. The properties demonstrated by these Ni:CuS thin films suggest their suitability for various optoelectronic applications, including optical coatings, photothermal applications, photosensors, and window layers for solar cell/photovoltaic devices.

Keywords: Nickel, Copper-Sulphide, Chalcogenides, Bandgap, Opto-electronics, Sol-gel, Dip-coating.

1.0 INTRODUCTION

The applications of most metal chalcogenide materials span vast areas, contributing to advancements in science and technology in recent times. These chalcogenides are compound semiconductor materials formed when metal ions react with group VI elements in the periodic table, except for oxygen, which typically forms oxides when combined with metal ions [1]. These compound materials possess the requisite characteristics for various applications, including energy generation and development, medicine, environmental protection, and military/security, addressing numerous human challenges [2-4].

Among the metal chalcogenides of interest are groups I-VI, II-VI, III-VI, and IV-VI, due to their unique characteristics [5]. Specifically, group I-VI compounds such as CuS, CuSe, CuTe, AgS, AgSe, and AgTe have attracted significant attention for energy generation and semiconductor device fabrication [6, 7]. CuS, a group I-VI chalcogenide semiconductor material, exhibits remarkable optical, electronic, and chemical properties, making it suitable for applications in photovoltaic cells, photosensors, energy storage, lithium-ion batteries, thermoelectric devices, and photocatalysis [8-10]. Naturally, the sulphides (Cu_xS) of copper crystallize into various phases, including chalcocite (Cu_2S), djurleite ($Cu_{1.96}S$), digenite ($Cu_{1.85}S$), anilite ($Cu_{1.75}S$), and covellite (CuS), with covellite being the most stable phase [11]. These phases of copper sulphide have significantly contributed to diverse applications. However, reports indicate that the formation of these phases into copper sulphide structures is complex and depends on multiple factors, including temperature variations. Its structure has been noted to be predominantly hexagonal and orthorhombic [12].

Incorporating elements such as transition metals and rare-earth metals into the crystal structure of copper sulphide through doping has shown promise in enhancing its performance for various device applications. Nickel, a transition metal,

International Multidisciplinary Research Journal Reviews (IMRJR)
A Peer-reviewed journal
Volume 1, Issue 4, December 2024
DOI 10.17148/IMRJR.2024.010405

exhibits remarkable properties, making it a suitable dopant for improving the performance of copper sulphide materials in device applications [13]. Studies have reported that the bandgap energy of Ni-doped CuS nanoparticles synthesized via a simple chemical co-precipitation technique decreases with increasing Ni doping content [14]. Additionally, Ni-doped CuS nanoparticles demonstrate enhanced photocatalytic activity compared to pristine CuS nanoparticles, with degradation efficiency improving as Ni concentration increases. Furthermore, nanofilms of Ni-doped CuS synthesized via the solvothermal route have exhibited significant changes in magnetic properties due to Ni doping [15].

Similarly, Ni-doped CuS nanoparticles deposited through a wet chemical co-precipitation approach have demonstrated strong ferromagnetism, with their optical bandgap red-shifting as Ni ion concentration increases [16]. The authors concluded that 2% and 4% Ni-doped CuS nanoparticles are suitable for spintronic device fabrication. Additionally, the impact of Ni doping on CuS nano-composite films as electrocatalysts for the oxygen evolution reaction (OER) has been investigated [17]. The authors concluded that 3% Ni-doped CuS was more effective for OER than pure CuS, based on their fabrication method and conditions.

In this study, the sol-gel dip-coating approach was employed to synthesize Ni-doped CuS thin films at different Ni ion concentrations to investigate their properties for fundamental applications, particularly in solar energy generation.

2.0 MATERIALS AND METHOD

In the preparation of the nickel-doped copper sulphide thin films, the materials and apparatus used were; microscopic glass substrates, digital weighing balance, glass beakers (100 mL, 250 mL and 500 ml), measuring cylinder (50 mL and 100 mL), electric oven and magnetic stirrer with hot plate and magnetic bead, while the precursors/reagent used include; copper (II) tetraoxosulphate (VI) as source for Cu^{2+} ions, sodium disulphide was used as source for S^{2-} ions and nickel (II) chloride hexahydrate as source of Ni^{2+}, while ethylene glycol was used as a stabilizing agent. The Sol-gel method was employed to synthesize the gel solution of the mixture of the precursors by firstly mixing 100 ml of 0.1 M copper (II) tetraoxosulphate (VI) and 10 ml of ethylene glycol solution in 250 mL glass beaker and stirring the mixture vigorously for 10 minutes. This was followed by the addition of 20 ml of 0.02 M nickel (II) chloride hexahydrate to the mixture and stirred for another 10 minutes before the final addition of 100 ml of 0.2 M sodium disulphide nanohydrate solution. The final solution was stirred for another 30 minutes to form a homogenous solution. The addition of sodium disulphide nanohydrate led to the formation of black precipitates which indicated that copper sulphide sol-gel was formed. The reactions between copper (II) tetraoxosulphate (VI), nickel (II) chloride hexahydrate and sodium disulphide nanohydrate for the formation of Ni-doped Copper Sulphide are given as

$$CuSO_4.8H_2O + Na_2S\,.9H_2O \rightarrow CuS + Na_2SO_4 + 17H_2O.$$

$$NiCl_2\,.6H_2O + Na_2S\,.9H_2O \rightarrow NiS + 2NaCl + 15H_2O$$

In the reactions, CuS and NiS combined to form nickel-doped copper sulphide gel solution. The gel was washed several times with distilled water to remove unwanted soluble compounds. Four other nickel-doped copper sulphide gel solutions were prepared using 20 ml of 0.04 M. 0.06 M, 0.08 M and 0.10 M of nickel (II) chloride hexahydrate solutions respectively and washed with distilled water. The washed nickel-doped copper sulphide gel solution was stored to be used for nickel-doped copper sulphide thin films via a dip coating approach on a microscopic glass substrate. Before the use of the substrates, they were degreased by washing with detergent and distilled water and allowed to dry. Five glass substrates each was dipped into the solution of each synthesis nickel-doped copper sulphide gel solution for 10 times to allow for the fabrication of Ni:CuS thin films on the glass substrates. The fabricated films were dried in an electric oven. The summary of the dip coating approach for the deposition of the Ni:CuS thin films on the glass substrate at varying concentrations of nickel ion precursor is displayed in Table 1.

Table 1: Number of dipping for deposition of nickel doped copper sulphide thin films

Baths Name	Concentration of Ni ion precursor (M)	Number of Dip Times
Ni(0.02 M)CuS	0.02	10
Ni(0.04 M)CuS	0.04	10
Ni(0.06 M)CuS	0.06	10
Ni(0.08 M)CuS	0.08	10
Ni(0.10 M)CuS	0.10	10

The fabricated thin films of Ni-doped CuS were characterized using x-ray diffraction method, UV-VIS spectroscopy, scanning electron microscopy/energy dispersive spectroscopy (SEM/EDS) technique to determine their structural, optical, morphological as well as compositional properties of the films for any desirable application.

International Multidisciplinary Research Journal Reviews (IMRJR)
International Multidisciplinary Research Journal Reviews (IMRJR)
A Peer-reviewed journal
Volume 1, Issue 4, December 2024
DOI 10.17148/IMRJR.2024.010405

3.0 RESULTS AND DISCUSSIONS

3.1 Film Thickness Measurement

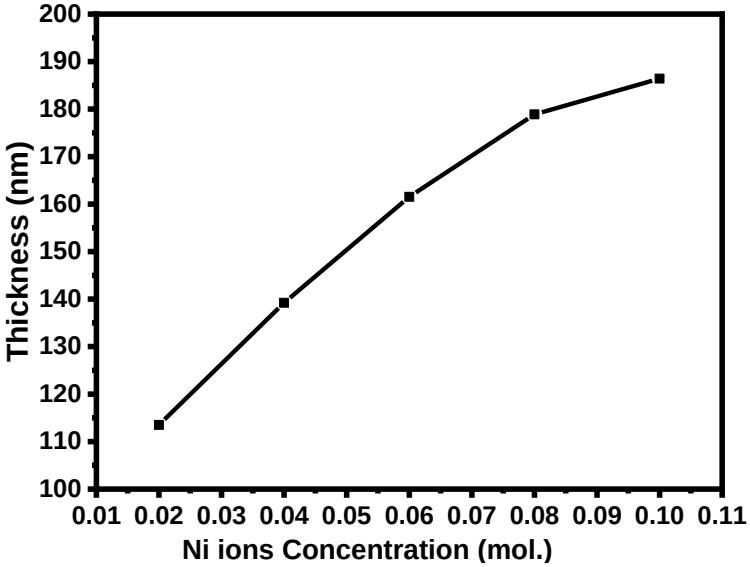

Figure 1: Graph of thickness plotted against concentration of Nickel ion precursor for the nickel-doped copper sulphide (Ni:CuS) thin films

Figure 1 shows the thickness graph plotted against nickel ion precursor concentration. The thickness of the films was determined using the gravimetric method as given by [18-21].

$$t = \frac{\Delta m}{\rho S} \qquad (1)$$

where Δm is the mass of the film, S is the surface area of the deposited film on the substrate and ρ is the bulk density of the material film. The masses of the deposited films were obtained by finding the difference in mass between the mass of the glass substrate after film deposition and the mass of the glass substrate before deposition. These differences in mass of the films were measured using a digital weighing balance with a sensitivity of 0.0001 g. From the graph, the thickness of the films increases as nickel ion concentration increases from 0.02 M to 0.10 M. The thickness of the films was found to range from 113.51 nm to 186.41 nm. This increase in film thickness due to an increase in the concentration of nickel ion precursor could be attributed to changes in the growth rate and chemical composition of the thin film materials. Similar increases in thickness as nickel concentration increases have been reported by [22-24].

3.2 Optical properties of nickel-doped copper sulphide (Ni:CuS) thin films

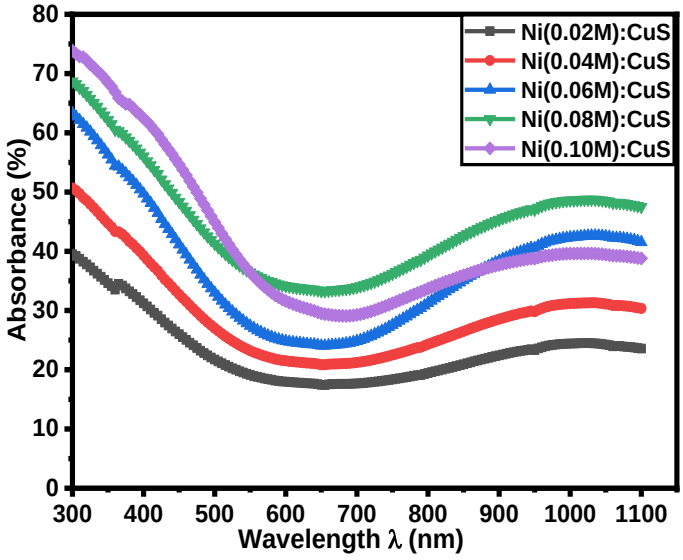

Figure 2: Absorbance graphs of nickel-doped copper sulphide thin films deposited at different concentrations of nickel ion precursor

International Multidisciplinary Research Journal Reviews (IMRJR)
A Peer-reviewed journal
Volume 1, Issue 4, December 2024
DOI 10.17148/IMRJR.2024.010405

Figure 2 shows the graph of absorbance of the deposited nickel-doped copper sulphide thin films plotted against wavelength. The graph showed that the percentage of absorbance of the films initially decreased as wavelength increases within UV and VIS regions but increased within NIR region. Absorbance was also found to increase as the concentration of nickel dopant increased. The copper sulphide thin film doped with 0.02 M of nickel ion dopant has absorbance values of 39.50% at 300 nm wavelength but decreased to 31.21% at 400 nm and further decreased to 17.44% at 655 nm and thereafter increased slightly to 23.57% as wavelength increased to 1100 nm. The thin film doped with 0.04 M of nickel ions has absorbance values of 50.68% at 300 nm which decreased to 39.28% at 400 nm wavelength and further decreased to 20.85% at 655 nm and then increased slightly to 30.35% at 1100 nm. The film doped with 0.06 M of nickel ion precursor has absorbance values of 63.29% at 300 nm (UV region) but decreased to 49.72% at 400 nm and further decreased to 24.05% at 655 nm (VIS region) and then increased slightly to 41.53% as wavelength increased to 1100 nm (NIR region). The copper sulphide thin film doped with 0.08 M of nickel ion precursor has an absorbance percent of 68.68% at 300 nm which decreased to 56.02% at 400 nm and further decreased to 33.49% at 655 nm and then increased slightly to 47.51% at 1100 nm. The film doped with 0.10 M of nickel ion precursor has the highest percentage of absorbance of 73.85% at 300 nm but decreased to 62.42% at 400 nm and further decreased to 29.08% at 685 nm (VIS region) and thereafter increased slightly to 38.81% at 1100 nm in the NIR region. The trend indicates that nickel doping enhances absorbance of CuS, particularly in the UV and NIR regions.

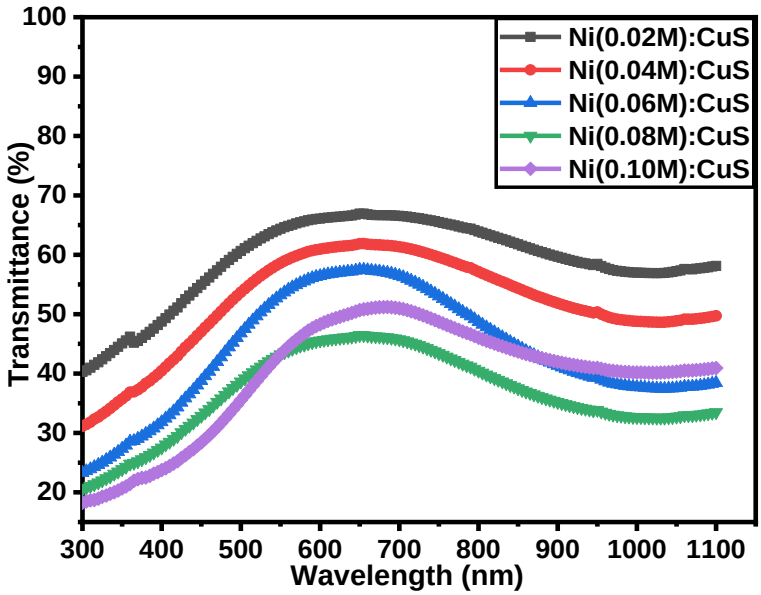

Figure 3: Transmittance graphs against wavelength for the nickel-doped copper sulphide thin films

Figure 3 shows the graph of transmittance of the deposited nickel-doped copper sulphide thin films plotted against wavelength. The transmittance of the films was evaluated using the relation given by [25, 26].

$$T = 10^{-A} \times 100 \quad (2)$$

Where A represents the measured absorbance value of the films.

From the graph, it was observed that the percentage transmittance of the films increased as wavelength increased within UV and VIS regions but decreased within the NIR region. The copper sulphide thin film doped with 0.02 M of nickel ion precursor has transmittance values of 40.28% at 300 nm which increased to 66.93% at 655 nm and then decreased slightly to 58.12% at 1100 nm. The one doped with 0.04 M of nickel ion precursor has transmittance values of 3113% at 300 nm and increased to 61.88% at 655 nm which then decreased slightly to 49.71% at 1100 nm. The film doped with 0.06 M of nickel ion has transmittance values of 23.29% at 300 nm but increased to 57.48% at 655 nm and thereafter decreased to 38.43% at 1100 nm. The copper sulphide thin film doped with 0.08 M of nickel ion precursor has a transmittance percent of 20.57% at 300 nm which increased to 46.46% at 655 nm but decreased to 33.49% at 1100 nm. The copper sulphide thin film doped with 0.10 M of nickel ion precursor has the lowest percentage transmittance values of 18.26% at 300 nm which increased to 23.76% at 400 nm and further increased to 51.20% at 685 nm but decreased slightly to 40.92% at 1100 nm. The transmittance of the films was also generally found to decrease as concentration of nickel increased except for the film doped with 0.10 M Ni which deviated from the trend in the NIR region.

International Multidisciplinary Research Journal Reviews (IMRJR)
A Peer-reviewed journal
Volume 1, Issue 4, December 2024
DOI 10.17148/IMRJR.2024.010405

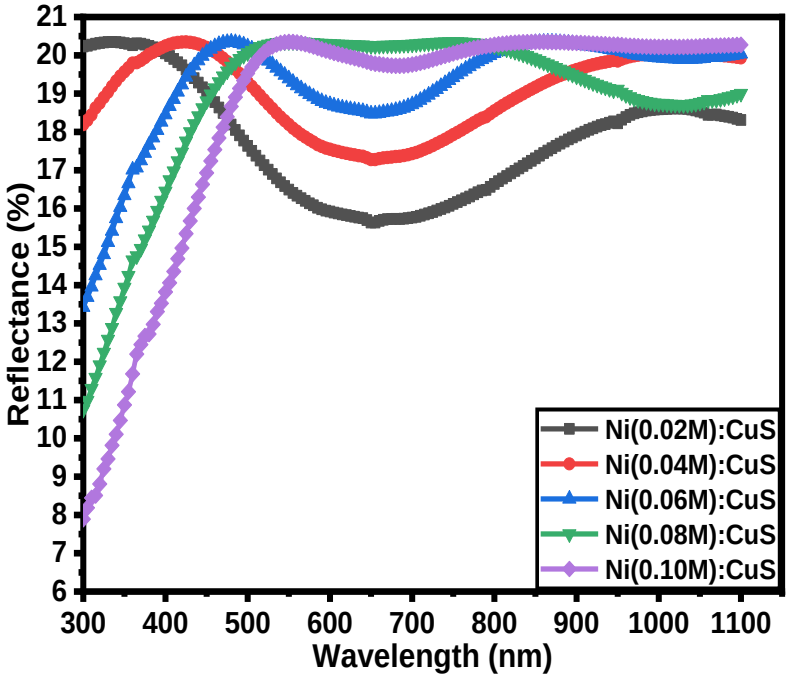

Figure 4: Reflectance graphs of nickel-doped copper sulphide thin films deposited at different concentrations of nickel ion precursor

Figure 4 represents the graph of reflectance of the deposited nickel-doped copper sulphide thin films against wavelength. The reflectance was calculated using the relation given by [27].

$$R = 1 - [T\, e^{A}]^{\frac{1}{2}} \qquad (3)$$

Where T is the transmittance of the films.

The percentage reflectance of the films according to the figure showed linear relationship existed between the reflectance and wavelength for the films in the UV region and an inverse relationship in the VIR region except for the film doped with 0.08 M Ni which showed a constant value but decreased in the NIR region. The films have low reflectance with maximum values of about 20.22% for all in the UV-VIS regions except for the films Ni(0.08M)CuS and Ni(0.10M)CuS which tend to maintain the 20.22% in VIS and NIR. The film doped with 0.02 M of nickel ion precursor has reflectance values that range from 15.76% to 20.22% in the UV-VIS/NIR regions. The film doped with 0.04 M of nickel ion precursor has reflectance values that range from 17.43% to 20.22% while the film doped with 0.06 M of nickel ion precursor has reflectance values that range from 13.42% to 20.04%. The copper sulphide thin film doped with 0.08 M of nickel ion precursor has reflectance values that range from 10.75% to 20.22%. The film doped with 0.10 M of nickel ion precursor has reflectance percentage values that range from 7.89% to 20.22%. The low reflectance values of the films suggest the suitable application of the films for anti-reflective coatings on the surfaces of materials such as surface of lenses, photovoltaic cells and other optical elements to reduce reflection. The variations in the reflectance of the deposited thin films nickel-doped CuS indicates that concentration of nickel ion precursor has effect on the film reflectance properties.

International Multidisciplinary Research Journal Reviews (IMRJR)
A Peer-reviewed journal
Volume 1, Issue 4, December 2024
DOI 10.17148/IMRJR.2024.010405

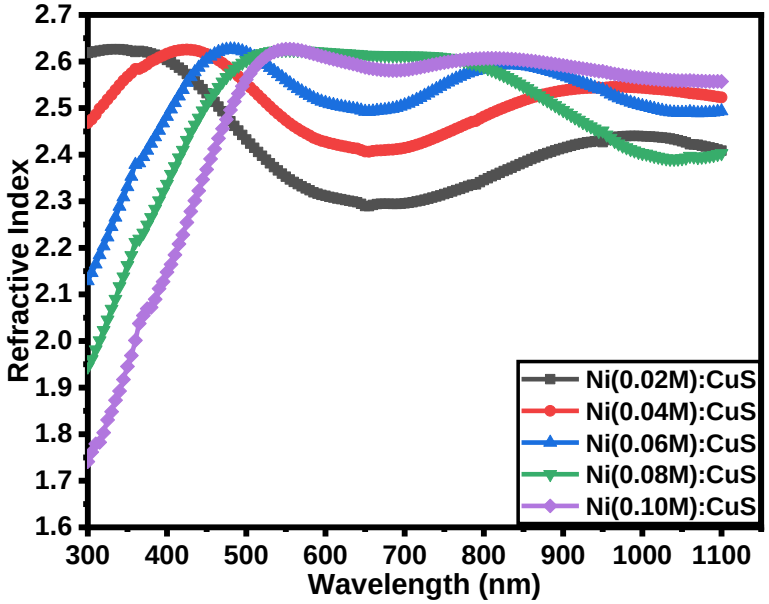

Figure 5: Refractive index graphs of nickel-doped copper sulphide thin films deposited at different concentrations of nickel ion precursor

Figure 5 shows the graph of the refractive index of the deposited thin films of nickel-doped copper sulphide plotted against wavelength. The refractive index of the films was determined using the formula provided by [28, 29].

$$\eta = \frac{1+R}{1-R} + \sqrt{\frac{4R}{(1-R)^2} - k^2} \qquad (4)$$

Where R is the reflectance of the films and k represents the extinction coefficient of the films

The figure indicates that the deposited thin films of nickel-doped copper sulphide exhibited high values of refractive index with the films doped with higher concentration of Ni showing linear relationship with wavelength in the UV-VIS regions. The films have maximum refractive index value of 2.62 within the UV-VIS regions. The range of values of refractive index for deposited thin films of nickel-doped CuS were found to be 2.30 to 2.62 for Ni(0.02M)CuS, 2.41 to 2.62 for Ni(0.04M)CuS, 2.13 to 2.62 for Ni(0.06M)CuS, 2.61 to 1.94 for Ni(0.08M)CuS and from 1.74 to 2.62 for the film Ni(0.10M)CuS. The high values of refractive index exhibited by the deposited thin films make them good materials for optical coating applications such as lens surface of lenses, optical fibre and other optical devices.

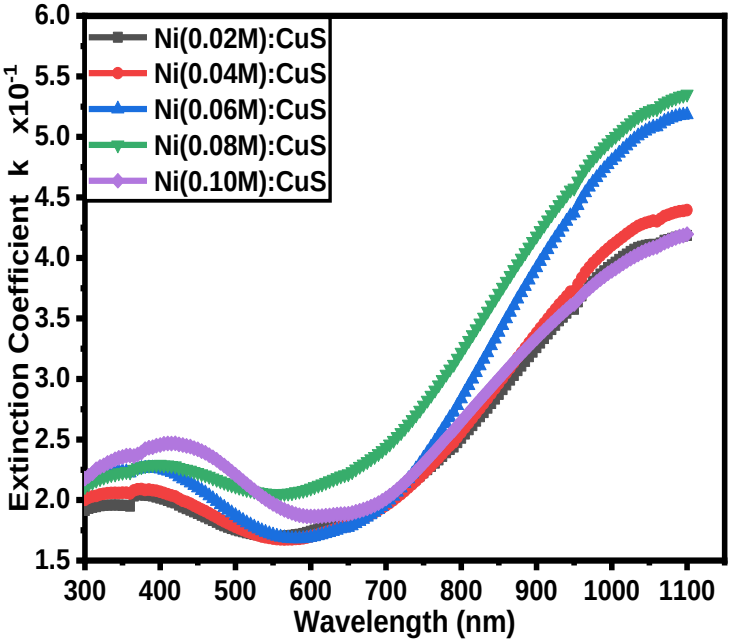

Figure 6: Extinction coefficient graphs of nickel-doped copper sulphide thin films deposited at different concentrations of nickel ion precursor

International Multidisciplinary Research Journal Reviews (IMRJR)
A Peer-reviewed journal
Volume 1, Issue 4, December 2024
DOI 10.17148/IMRJR.2024.010405

Figure 6 shows the graph of the extinction coefficient of the deposited nickel-doped copper sulphide thin films plotted against wavelength. The extinction coefficient was obtained using the relation as provided by [30-32].

$$k = \frac{\alpha \lambda}{4\pi} \quad (5)$$

The results showed that extinction coefficient values increased as wavelength increased. The extinction coefficient was found not to have a linear relationship with the concentration of nickel ions in the VIS and NIR regions but in the UB-VIS, the films showed a linear relation. The film doped with 0.02 M Ni ions has extinction coefficient values that ranged between 1.91×10^{-1} and 4.19×10^{-1}. The film doped with 0.04 M of nickel ions has extinction coefficient values that ranged between 2.00×10^{-1} and 4.40×10^{-1} while the film doped with 0.06 M of nickel ions values in the range of 2.15×10^{-1} to 5.18×10^{-1}. On the other hand, the film doped with 0.08 M of nickel ions has extinction coefficient values that range between 2.11×10^{-1} and 5.35×10^{-1}while the film doped with 0.10 M of nickel ions has extinction coefficient values that range between 2.18×10^{-1} and 4.20×10^{-1}. This different in the values of extinction coefficient for the deposited thin films showed that variation of concentrations of the Ni ions have effect on the extinction coefficient properties and thus position the films for many optoelectronic applications.

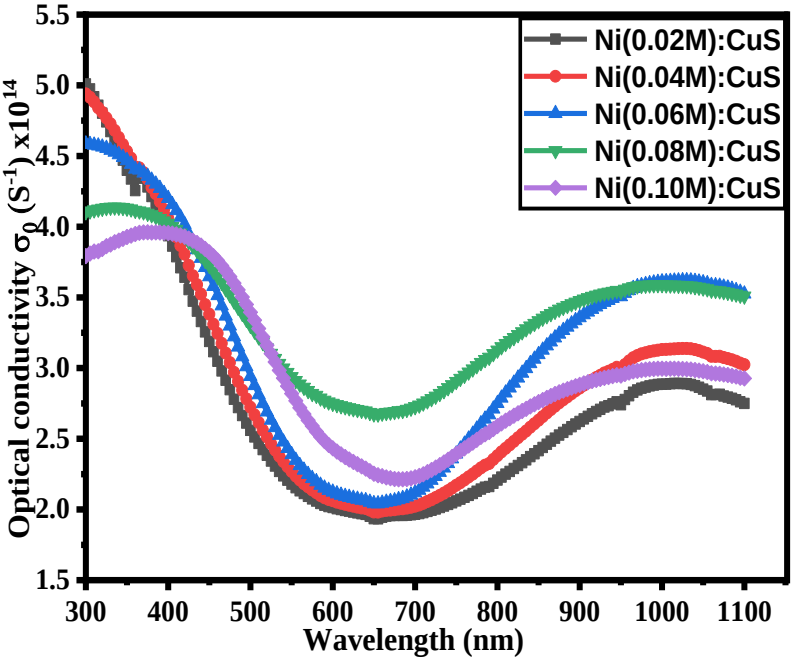

Figure 7: Optical conductivity graphs of nickel doped copper sulphide thin films deposited at different concentration of nickel ion precursor

Figure 7 shows the graph of optical conductivity of the deposited nickel doped copper sulphide thin films plotted against wavelength. The results showed that optical conductivity values of the films decreased as wavelength increases within UV and VIS regions but increased within NIR region. Optical conductivity was obtained using the relation as given by [33-35].

$$\sigma_o = \frac{\alpha \eta c}{4\pi} \quad (6)$$

Where α is the absorption coefficient, η is the refractive index and c is the speed of light in vacum. From the graph, it was found that the optical conductivity of the films decreased with wavelength in the UV-VIS regions but increased in the NIR. In the UV region, the optical conductivity of the films decreased as concentration of Ni ions increased. However, the trend was not maintained in the VIS and NIR regions. The film doped with 0.02 M of nickel ions has optical conductivity values of $5.01 \times 10^{14}\ s^{-1}$ at 300 nm which decreased to the value of $3.94 \times 10^{14}\ s^{-1}$at 400 nm wavelength and further decreased to $1.93 \times 10^{14}\ s^{-1}$ at 655 nm and thereafter increased slightly to $2.75 \times 10^{14}\ s^{-1}$ at 1100 nm. The film doped with 0.04 M of nickel ion has optical conductivity values of $4.94 \times 10^{14}\ s^{-1}$ at 300 nm which decreased to $4.06 \times 10^{14}\ s^{-1}$ at 400 nm and further decreased to minimum value of $1.98 \times 10^{14}\ s^{-1}$ at 655 nm and then increased slightly to $3.02 \times 10^{14}\ s^{-1}$ at 1100 nm. The film doped with 0.06 M of nickel ions has optical conductivity values of $4.59 \times 10^{14}\ s^{-1}$ at 300 nm which decreased to $4.20 \times 10^{14}\ s^{-1}$ at 400 nm and further decreased to $2.04 \times 10^{14}\ s^{-1}$ at 655 nm and then increased slightly to $3.52 \times 10^{14}\ s^{-1}$ at 1100 nm. The copper sulphide thin film doped with 0.08 M of nickel ions has optical conductivity values of $4.11 \times 10^{14}\ s^{-1}$ at 300 nm that decreased to $4.02 \times 10^{14}\ s^{-1}$ at 400 nm and further decreased to $2.67 \times 10^{14}\ s^{-1}$ at 655 nm and then increased slightly to $3.51 \times 10^{14}\ s^{-1}$ at 1100 nm. Finally,

International Multidisciplinary Research Journal Reviews (IMRJR)
A Peer-reviewed journal
Volume 1, Issue 4, December 2024
DOI 10.17148/IMRJR.2024.010405

the film doped with 0.10 M of nickel ions has optical conductivity values of $3.79 \times 10^{14}\ s^{-1}$ at 300 nm which decreased to $3.95 \times 10^{14}\ s^{-1}$ at 400 nm and further decreased to $2.22 \times 10^{14}\ s^{-1}$ at 685 nm and then increased to the value of $2.93 \times 10^{14}\ s^{-1}$ at 1100 nm.

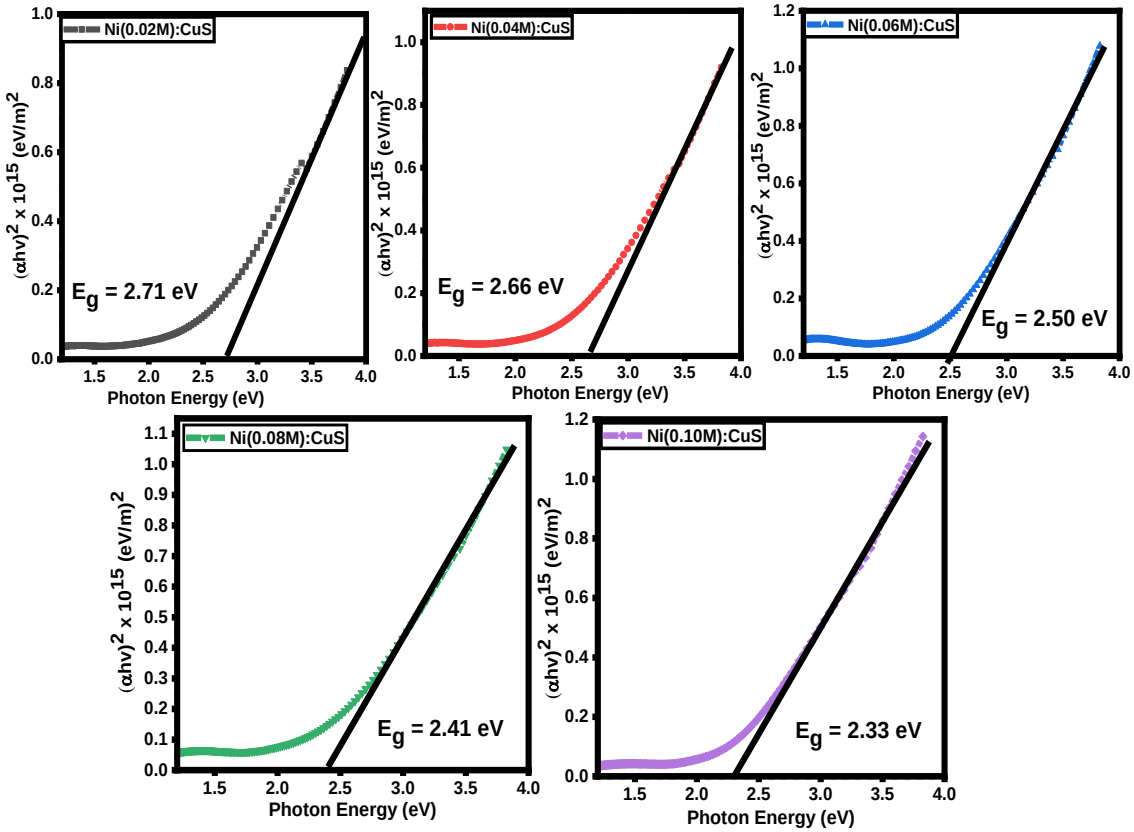

Figure 8: Plot of $(\alpha hv)^2$ against photon energy for nickel-doped copper sulphide thin films deposited at different concentrations of nickel ion precursor

Figure 8 shows the plots of $(\alpha hv)^2$ against photon energy for the deposited nickel-doped copper sulphide thin films at different concentrations of nickel ion precursor to determine the bandgap energy of the films. The plots were made based on Tauc's model as provided by [36, 39]

$$(\alpha hv)^n = \beta\left(hv - E_g\right) \tag{7}$$

where β is a constant known as energy shape factor, n is a transition factor which has value of 2 for direct transition and ½ for indirect transition and E_g is the bandgap energy of material of interest. From the plots, energy bandgaps of the films were estimated by extrapolation of the straight portion of the graph along the photon energy axis where $(\alpha hv)^2 = 0$. Energy band gap of 2.71 eV was obtained for the thin films deposited with 0.02 M of nickel ion. Energy bandgaps of 2.66 eV, 2.50 eV, 2.41 eV and 2.33 eV were obtained for the films doped with 0.04M, .0.06M, 0.08M and 0.10M of nickel ions respectively. The result showed a decrease in the bandgap energy of the films as the concentration of nickel ions increased. This confirmed the likelihood of tuning the energy band gap of copper sulphide by varying nickel ion concentration as dopant. Similar effect of dopant concentration on the band gap of thin film materials had been reported by [40, 41]. The increase in nickel ion concentration gave rise to increase in the films thickness and decrease in energy band gap which is likely to be attributed to quantum confinement effect.

International Multidisciplinary Research Journal Reviews (IMRJR)
A Peer-reviewed journal
Volume 1, Issue 4, December 2024
DOI 10.17148/IMRJR.2024.010405

3.3 Structural properties of nickel doped copper sulphide (Ni:CuS) thin films

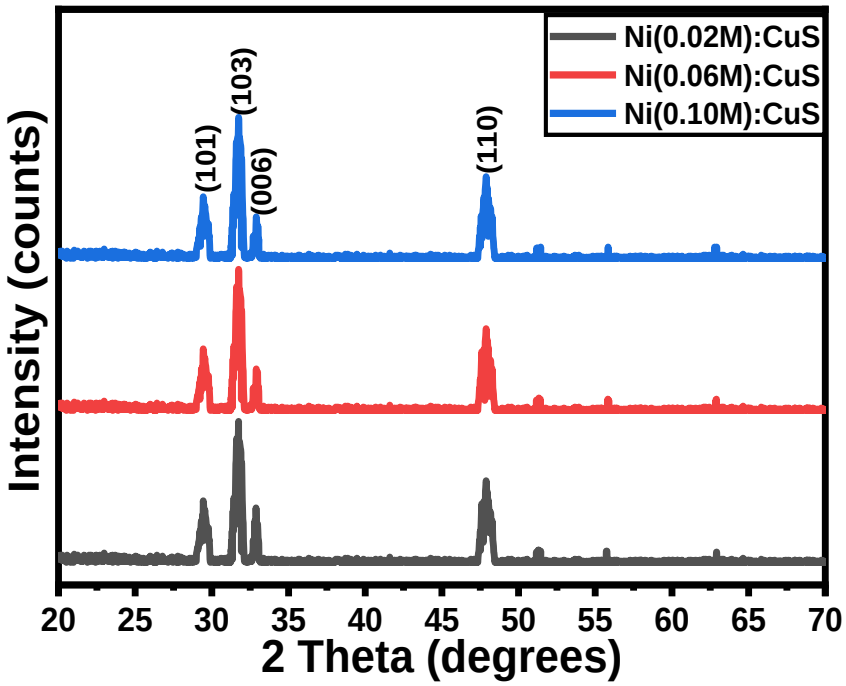

Figure 9: XRD spectra of nickel-doped copper sulphide thin films deposited at different concentrations of nickel ion precursor

Figure 9 shows the XRD spectrum of nickel-doped copper sulphide thin films deposited at different concentrations of nickel ion precursor. The nickel-doped copper sulphide thin film deposited with 0.02 M of nickel ion precursor has diffraction peaks at 29.48 °, 31.72 °, 32.90 ° and 47.90 ° The thin film doped with 0.06 M of nickel ion precursor has diffraction peaks at 29.49 °, 31.73 °, 33.00 ° and 47.89 ° while the film deposited with 0.10 M of nickel ion dopant has diffraction peaks at 29.55 °, 31.76 °, 33.04 ° and 48.05 °. These diffraction peaks for the synthesized thin films nickel-doped copper sulphide matched well with the standard JCPDS file number (00-006-0464) for CuS with mineral name covellite and hexagonal phase structure. These two theta angles corresponded to the crystalline planes (101), (103), (006) and (110) as depicted in figure 9. Ni-CuS thin films with similar structures deposited hydrothermal method has been reported by [42]. The average crystallite sizes (D), dislocation density and micro-strain of the films were calculated using the Debye-Scherrer and Williamson-Smallman relations as provided by [43, 44]

$$D = \frac{0.9\lambda}{\beta Cos\theta} \quad (8)$$

$$\delta = \frac{1}{D^2} \quad (9)$$

$$\varepsilon = \frac{\beta}{4*Tan\theta} \quad (10)$$

Where λ is the probing x-ray wavelength, β is the full-width half maximum (FWHM), θ is the Bragg's angle.

The crystallite size for the films doped with 0.02 M, 0.06 M and 0.1 M nickel ions dopant was found to be 19.45 nm, 19.54 nm and 19.92 nm respectively. The overall average dislocation density of the films doped with 0.02 M, 0.06 M and 0.10 M Ni dopant were calculated to be $3.359x10^{-3}$ nm^{-2} $3.24\ x10^{-3}$ nm^{-2} and $3.179x10^{-3}$ nm^{-2} respectively, while the micro-strain were found to be $6.494x10^{-3}$, $6.378x10^{-3}$ and $6.319x10^{-3}$ respectively. The crystallite size values of the films were found to increase as the concentration of nickel ions increased. [45].

International Multidisciplinary Research Journal Reviews (IMRJR)
A Peer-reviewed journal
Volume 1, Issue 4, December 2024
DOI 10.17148/IMRJR.2024.010405

3.4 Morphological analysis of nickel-doped copper sulphide (Ni:CuS) thin films

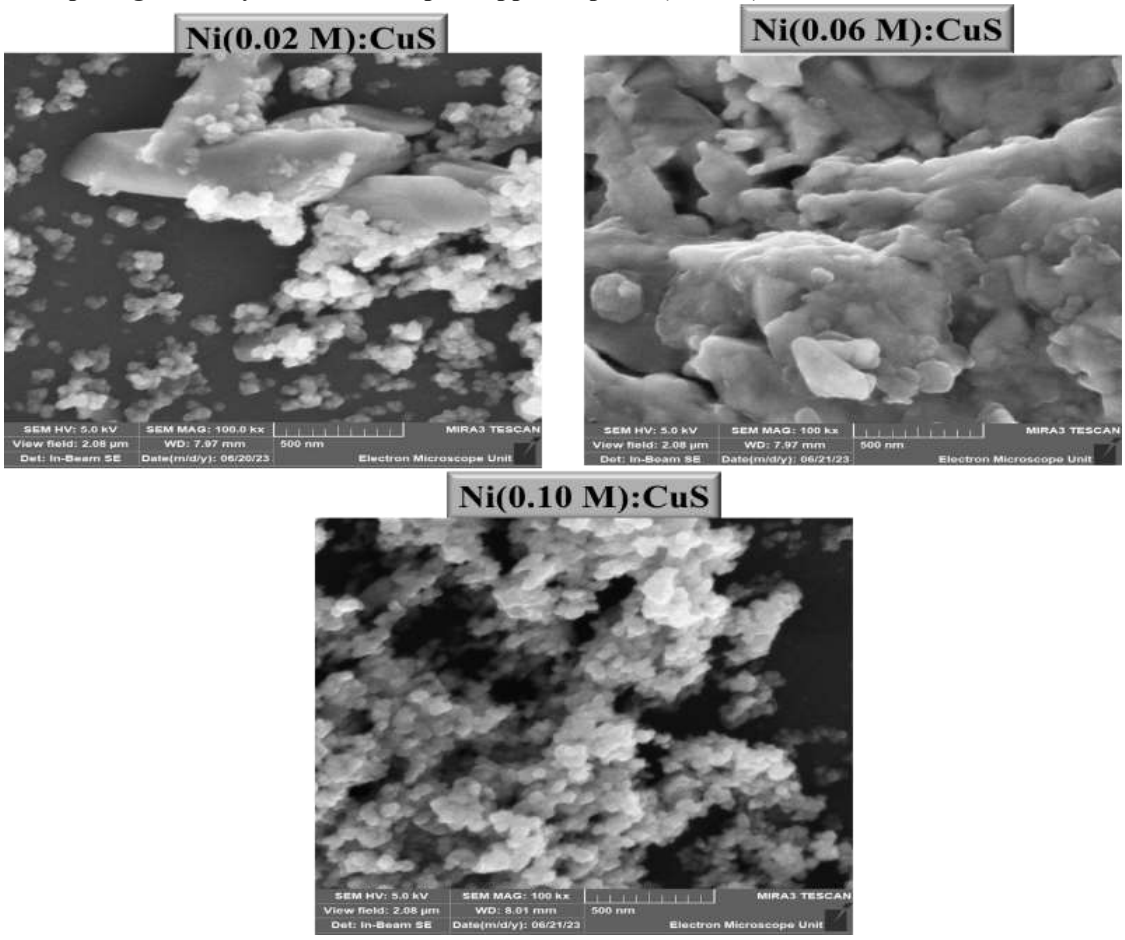

Figure 10: Micrographs of nickel-doped copper sulphide thin films deposited at different concentrations of nickel ion precursor

Figure 10 shows the micrograph of nickel-doped copper sulphide thin films deposited at different concentrations of nickel ion precursor. The micrograph shows that the particles of the deposited films are spherical. However, agglomerations of lump particles were noticed in the films deposited with 0.02 M and 060 M of Ni ions. The analysis of the micrographs done using ImageJ software showed that the films composed of a nanosphere with particle sizes of 82.91 nm, 89.11 nm and 94.10 nm for 0.02 M, 0.06 M and 0.10 M Ni doped CuS thin films respectively. This result indicates that the particle size of the films increased as the concentration of nickel ions increased.

3.5 Compositional analysis of nickel-doped copper sulphide (Ni:CuS) thin films

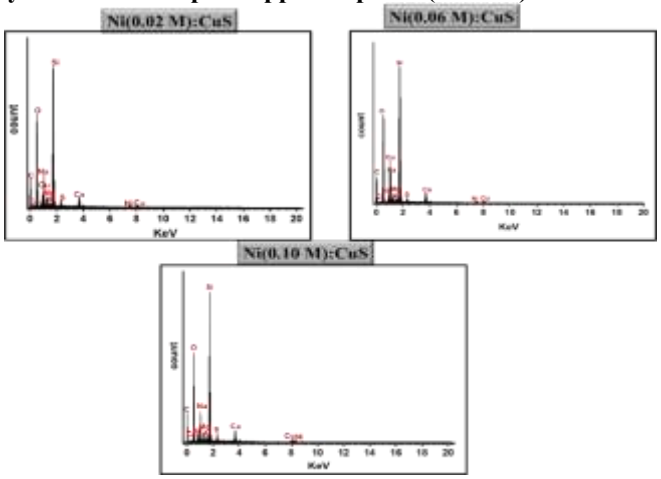

Figure 11: EDS spectra of nickel-doped copper sulphide thin films deposited at different concentrations of nickel ion precursor

International Multidisciplinary Research Journal Reviews (IMRJR)
A Peer-reviewed journal
Volume 1, Issue 4, December 2024
DOI 10.17148/IMRJR.2024.010405

Figure 11 shows the EDS spectra of the deposited thin films of Ni-doped CuS to determine the elemental composition of the films for different concentrations of nickel ion precursor. The EDS spectra showed the presence of the desired element; copper (Cu), nickel (Ni) and sulphur (S) in addition to other elements present in the films as shown in Table 2 with their atomic percentage values. This result confirms the presence of the desired elements in the deposited thin films. The absorbance of the films was found to increase with an increase in the Ni concentration while percentage transmittance decreased as the Ni concentration increased.

Table 2: Elemental Composition of nickel-doped copper sulphide thin films

Elements												
Bath Name		**C**	**O**	**Na**	**Mg**	**Al**	**Si**	**S**	**Ca**	**Ni**	**Cu**	**Total**
Ni(0.02 M): CuS	Atomic %	4.56	26.74	7.80	1.78	0.59	20.44	1.94	3.20	4.44	28.51	100
Ni(0.06 M): CuS		3.79	25.31	8.44	1.43	0.45	19.60	1.01	3.16	6.34	30.47	100
Ni(0.10 M): CuS		6.33	24.21	7.17	1.59	0.38	15.2	2.82	3.03	8.18	31.09	100

CONCLUSION

In conclusion, the properties of Ni:CuS thin films deposited by sol-gel dip coating method were investigated using UV-Vis spectroscopy, x-ray diffraction technique, scanning electron microscopy and energy dispersive spectroscopy techniques for possible device applications. The analysis showed that Ni doping has a desirable effect on the optical and structural properties of the deposited thin films. The thickness of the deposited films was found to increase as nickel ion concentration increased from 0.02 M to 0.10 M and the thickness ranged from 113.51 nm to 186.41 nm. This phenomenon could be attributed to changes in the growth rate and chemical composition of the thin film materials. The absorbance of the films was found to increase with an increase in the concentration of Ni dopant while percentage transmittance showed a decrease in value as Ni concentration increased. The films exhibit high values of refractive index and the values were found to be highly dependent on the concentration of Ni ions throughout the UV-VIS and NIR regions. The obtained values of bandgap energies for the films were found to be red-shifted in the order of 2.66 eV, 2.50 eV, 2.41 eV and 2.33 eV for the films doped with 0.04M, .0.06M, 0.08M and 0.10M of nickel ions respectively. This showed that the bandgap of CuS can be tuned by varying nickel ion concentration as a dopant. This correlates to an increase in the film thickness as a result of Ni doping and the decrease in band gap energy value can be attributed to the quantum confinement effect in the films. The structural analysis results indicate that the films possess a crystalline structure with an average crystallite size of 19.45 nm, 19.54 nm and 19.92 nm for the films doped with 0.02 M, 0.06 M and 0.1 M nickel ions respectively. The average dislocation density of the films doped with 0.02 M, 0.06 M and 0.10 M Ni dopant were calculated to be 3.359×10^{-3} nm^{-2} 3.24×10^{-3} nm^{-2} and 3.179×10^{-3} nm^{-2}, while the micro-strains were found to be 6.494×10^{-3}, 6.378×10^{-3} and 6.319×10^{-3} respectively.

Conflict of Interest

The authors declared no conflict of interest during the research work.

REFERENCES

[1] Aghad, N., Narjis, A., Amiri, L., Elmassi, S., Alofi, A. S., Nkhaili, L., ... & Outzourhit, A. (2024). Phase transition, structural, optical and thermoelectric properties of spin coated CuxS thin films. *Physica B: Condensed Matter*, *673*, 1-7. https://doi.org/10.1016/j.physb.2023.415506

[2] Kadarwati, L. V., Lin, I. H., Huang, Y. S., Lee, Y. Y., Chen, S. C., Chung, C. L., ... & Kuo, T. R. (2024). Exploring Label-Free Imaging Techniques with Copper Sulfide Microspheres for Observing Breast Cancer Cells. *ACS omega*, *9*(36), 37882-37890. https://doi.org/10.1021/acsomega.4c04154

[3] Huang, J., Zhou, J., Zhuang, J., Gao, H., Huang, D., Wang, L., … Han, M.-Y. (2017). *Strong Near-Infrared Absorbing and Biocompatible CuS Nanoparticles for Rapid and Efficient Photothermal Ablation of Gram-Positive and -Negative Bacteria. ACS Applied Materials & Interfaces, 9(42), 36606–36614.* doi:10.1021/acsami.7b11062

[4] Elekalachi, C., Ezenwa, . I. A., Okereke, N. A., Okoli, N. L., & Nwori, A. N. (2024). Thermal Annealing Impact on the Properties of CdSe/PbSe Superlattice Thin Films: CdSe/PbSe Superlattice Thin Films. *OAJ Materials and Devices*, *8*. 1-13. Retrieved from https://www.co-ac.com/caip/index.php/materialsanddevices/article/view/176

[5] Obata, K., Higashi, T., Hasegawa, M., Katayama, M., & Takanabe, K. (2022). Synthesis of Metal Chalcogenide Semiconductors by Thermal Decomposition of Organosulfur and Organoselenium Compounds. *Chemistry–A European Journal*, *28*(61), 1-8. https://doi.org/10.1002/chem.202201951

[6] Kapuria, N., Ghorpade, U. V., Zubair, M., Mishra, M., Singh, S., & Ryan, K. M. (2020). Metal chalcogenide semiconductor nanocrystals synthesized from ion-conducting seeds and their applications. *Journal of Materials Chemistry C*, *8*(40), 13868-13895. doi:10.1039/d0tc02895a

International Multidisciplinary Research Journal Reviews (IMRJR)
A Peer-reviewed journal
Volume 1, Issue 4, December 2024
DOI 10.17148/IMRJR.2024.010405

[7] Muomeliri, C. B., Okereke, N. A., Nwori, A. N., Okpala, U. V., & Okoli, N. L. (2024). Electrosynthesis and Characterizations of Aluminum Silver Selenide (Alagse2), Thin Films for Possible Device Applications. *International Journal of Research and Scientific Innovation*, *11*(9), 954-961. https://doi.org/10.51244/IJRSI.2024.110908
[8] Çayır Taşdemirci, T. (2019). *Study of the physical properties of CuS thin films grown by SILAR method. Optical and Quantum Electronics, 51(7).* doi:10.1007/s11082-019-1963-0
[9] Omran, A. H., & Jaafer, M. D. (2013). Annealing effect on the structural and optical properties of CuS thin film prepared by Chemical Bath Deposition (CBD). *Journal of Kufa-physics*, *5*(1), 80-90.
[10] Diliegros-Godines, C. J., Lombardero-Juarez, D. I., Machorro-Mejía, R., González, R. S., & Pal, M. (2019). *Electrical properties and spectroscopic ellipsometry studies of covellite CuS thin films deposited from non-ammoniacal chemical bath. Optical Materials, 91, 147–154.* doi:10.1016/j.optmat.2019.03.022
[11] Mukherjee, N., Sinha, A., Khan, G. G., Chandra, D., Bhaumik, A., & Mondal, A. (2011). *A study on the structural and mechanical properties of nanocrystalline CuS thin films grown by chemical bath deposition technique. Materials Research Bulletin, 46(1), 6–11.* doi:10.1016/j.materresbull.2010.10.004
[12] Ghribi, F., Alyamani, A., Ayadi, Z. B., Djessas, K., & Mir, L. E. (2015). *Study of CuS Thin Films for Solar Cell Applications Sputtered from Nanoparticles Synthesised by Hydrothermal Route. Energy Procedia, 84, 197–203.* doi:10.1016/j.egypro.2015.12.314
[13] Sreelekha, N., Subramanyam, K., Amaranatha Reddy, D., Murali, G., Rahul Varma, K., & Vijayalakshmi, R. P. (2016). *Efficient photocatalytic degradation of rhodamine-B by Fe doped CuS diluted magnetic semiconductor nanoparticles under the simulated sunlight irradiation. Solid State Sciences, 62, 71–81.* https://doi.org/10.1016/j.solidstatesciences.2016.11.001
[14] Subramanyam, K., Sreelekha, N., Amaranatha Reddy, D., Murali, G., Rahul Varma, K., & Vijayalakshmi, R. P. (2017). *Chemical synthesis, structural, optical, magnetic characteristics and enhanced visible light active photocatalysis of Ni doped CuS nanoparticles. Solid State Sciences, 65, 68–78.* https://doi.org/10.1016/j.solidstatesciences.2017.01.008
[15] Wang, Z.-H., Geng, D.-Y., Zhang, Y.-J., & Zhang, Z.-D. (2010). *CuS:Ni flowerlike morphologies synthesized by the solvothermal route. Materials Chemistry and Physics, 122(1), 241–245.* doi:10.1016/j.matchemphys.2010.0
[16] Almohammedi, A. (2023). Structural, optical and magnetic properties of nickel-doped copper sulphide diluted magnetic semiconductor nanoparticles for spintronic devices. *Applied Physics A*, *129*(3), 221. https://doi.org/10.1007/s00339-023-06511-6
[17] Kundu, J., Khilari, S., Bhunia, K., & Pradhan, D. (2019). *Ni-doped CuS as an Efficient Electrocatalyst for Oxygen Evolution Reaction. Catalysis Science & Technology.* https://doi.org/10.1039/C8CY02181C
[18] Gode, F.& Unlu, S. (2018). Nickel doping effect on the structural and optical properties of indium sulfide thin films by SILAR, *Open Chemistry,* 16, 757 – 762. https://doi.org/10.1515/chem-2018-0089
[19] Chaudhary, P. & Kumar, V. (2019). Preparation of ZnO thin film using sol-gel dip-coating technique and their characterization for optoelectronic applications. *World Scientific News*, 121, 64 – 71.
[20] Nwori, A. N., Ezenwaka, L. N., Ottih, I. E., Okereke, N. A., & Okoli, N. L. (2022). Study of the optical, structural and morphological properties of electrodeposited copper manganese sulfide (CuMnS) thin films for possible device applications. *Trends in Sciences*, *19*(17), 5747-5747. https://doi.org/10.48048/tis.2022.5747
[21] Nwori, A. N., Okoli, N. L., Okereke, N. A., Ottih, I. E., & Ezenwaka, L. N. (2022). Optical Properties of Electrodeposited CdMnS Thin Film Semiconductor Alloys for Optoelectronics Applications: Effect of Deposition Potential. *Journal of Nano and Materials Science Research*, *1*, 58-67. https://doi.org/10.20221/jnmsr.v1i.7
[22] Owoeye, A. V., Ajenifuja, E., Adeoye, A. E., Osinkolu, A. G., & Popoola, A. P. (2019). Microstructural and optical properties of Ni-doped ZnO thin films prepared by chemical spray pyrolysis technique. *Materials Research Express,* 6(086455), 1-9. DOI 10.1088/2053-1591/ab26d9
[23] Osuwa, J. C. & Mgbaja, E. C. (2014) Structural and Electrical Properties of Copper Sulfide (CuS) Thin Films doped with Mercury and Nickel impurities. Journal of Applied Physics, 6(5), 28-31.
[24] Khan, M., Alam M. S. & Ahmed, S. F. (2023). Effect of nickel incorporation on structural and optical properties of zinc oxide thin films deposited by RF/DC sputtering technique. *Materials Physics and Mechanics*, 51(1), 19-32. http://dx.doi.org/10.18149/MPM.5112023_3
[25] Lokhande, C. D., Sankapal, B. R., Mane, R. S., Pathan, H. M., Muller, M., Giersig, M. & Ganesan, V. (2002). XRD, SEM, AFM, HRTEM, EDAX and RBS studies of chemically deposited Sb $_2S_3$ and Sb_2Se_3 thin films. *Applied Surface Science*, 193(1), 1 – 10. https://doi.org/10.1016/S0169-4332(01)00819-4
[26] Ismail, B., Mushtaq, S. & Khan A. (2014). Enhanced Grain Growth in the Sn Doped Sb_2S_3 Thin Film Absorber Materials for Solar Cell Applications. *Chalcogenide Letters,* 11(1), 37 – 45.
[27] Augustine, C., Nnabuchi, M. N., Chikwenze, R. A., Anyaegbunam, F. N. C., Kalu, P. N., Robert, B. J., Nwosu, C. N., Dike, C. O. & Taddy, E. N. (2019). Comparative investigation of some selected properties of Mn_3O_4/PbS and CuO/PbS composites thin films. *Material Research Express,* 6 (066416), 1 – 10. DOI 10.1088/2053-1591/ab1058
[28] Guneri, E., (2019). The Role of Au Doping on the Structural and Optical Properties of Cu_2O Films. *Journal of Nano Research,* 58, 49 – 67. https://doi.org/10.4028/www.scientific.net/JNanoR.58.49

International Multidisciplinary Research Journal Reviews (IMRJR)
A Peer-reviewed journal
Volume 1, Issue 4, December 2024
DOI 10.17148/IMRJR.2024.010405

[29] Murali, D. S. & Aryasomayajula, S. (2018). Thermal conversion of Cu_4O_3 into CuO and Cu_2O and the electrical properties of magnetron sputtered Cu_4O_3 thin films. *Apllied Physics A: Materials Science and Processing*, 124 (3), 1 – 7. https://doi.org/10.1007/s00339-018-1666-6

[30] Kariper, I. A. (2017). Synthesis and characterization of CrSe thin film produced via chemical bath deposition. *Optical Review*, 24(2), 139 – 146. https://doi.org/10.1007/s10043-017-0307-1

[31] Kalu, U. A., Okpala U.V, Okereke N. A & Nwori A. N. (2023). Structural and Optical Properties of Black Velvet Tamarind Doped Magnesium Sulfide Thin Films Grown by Sol-Gel Technique. Journal of Physics and Chemistry of Materials Vol.10, Issue.4, pp.01-09, December 2023 E-ISSN: 2348-6341 Available online at: www.isroset.org

[32] Tezel, F. M., Ozdemir, O. & Kariper, I. A. (2017). The Effects of pH on Structural and Optical Characterization of Iron Oxide Thin Films. *Surface Review and Letters*, 24(4), 1750051: 1 – 10. https://doi.org/10.1142/S0218625X17500512

[33] Ongwen, N. O., Oduor, A. O. & Ayieta, E. O. (2019). Effect of Concentration of Reactants on the Optical Properties of Iron–Doped Cadmium Stannate Thin Films Deposited by Spray Pyrolysis. *American Journal of Materials Science*, 9(1): 1-7.

[34] Sreedev, P., Rakhesh, V. & Roshina N. S., (2018). Optical Characterization of ZnO thin Films Prepared by Chemical Bath Deposition Method. *IOP Conf. Series: Materials Science and Engineering,* 377(012086): 1 – 7. DOI 10.1088/1757-899X/377/1/012086

[35] Mahrov, B., Boschloo, G., Hgfeldt, A., Dloczuk, L. & Dittrich, T., (2004), Photovoltage Study of Charge Injection from Dye Molecules into Transparent Hole and Electron Conductors, *Applied Physics Letters*, 84(26), 5455 – 5457. https://doi.org/10.1063/1.1767961

[36] Mushtaq, S., Ismail, B., Raheel, M. & Zeb, A. (2016). Nickel Antimony Sulphide Thin Films for Solar Cell Application: Study of Optical Constants. *Natural Science*, 8, 33-40. DOI: 10.4236/ns.2016.82004

[37] Ohwofosirai, A., Femi, M. D., Nwokike, A. N., Toluchi, O. J., Osuji, R. U. & Ezekoye, B. A. (2014). Study of the Optical Conductivity, Extinction Coefficient and Dielectric Function of CdO by Sucessive Ionic Layer Adsorption and Reaction (SILAR) Techniques. *American Chemical Science Journal,* 4(6), 736 – 744.

[38] Tauc, J., Grigorovici, R., & Vancu, A. (1966). Optical Properties and Electronic Structure of Amorphous Germanium. *Phys. Status Solidi,* 15(2), 627 – 637. https://doi.org/10.1002/pssb.19660150224

[39] Nwori, A. N., Ezenwaka, N. L., Ottih, I. E., Ngozi, A. O., & Okoli, N. L. (2021). Study of the Optical, Electrical, Structural and Morphological Properties of Electrodeposited Lead Manganese Sulphide (PbMnS) Thin Film Semiconductors for Possible Device Applications. *Journal of Modern Materials*, *8*(1), 40-51. https://doi.org/10.21467/jmm.8.1.40-51

[40] Ahmed, M., Alshahriea, A. & Shaaban, E. R. (2023). Films of copper sulphide doped with nickel for optoelectronics: structural, optical, and magnetic characteristics. *Chalcogenide Letters*, 20(9), 663 – 675. https://doi.org/10.15251/CL.2023.209.663

[41] Subramanyam, K., Sreelekha, N., Amaranatha Reddy, D., Murali, G., Rahul Varma, K., & Vijayalakshmi, R.P. (2017). Chemical synthesis, structural, optical, magnetic characteristics and enhanced visible light active photocatalysis of Ni doped CuS nanoparticles. Solid State Sciences, 65, 68-78. https://doi.org/10.1016/j.solidstatesciences.2017.01.008

[42] Selma M. H. AL-Jawad, Ali A. Taha, and Abdulah Mohammed Redha 2019). Studying the structural, morphological, and optical properties of CuS:Ni nanostructure prepared by a hydrothermal method for biological activity. Journal of Sol-Gel Science and Technology, 91:310–323. https://doi.org/10.1007/s10971-019-05023-1

[43] Aghad, N., Narjis, A., Amiri, L., Elmassi, S., Alofi, A. S., Nkhaili, L., Alsaad, A., Tihane, A., Karmouch, R., Albalawi, H., & Outzourhit, A. (2024). Phase transition, structural, optical and thermoelectric properties of spin-coated Cu_xS thin films. Physica B: Condensed Matter, 673, 415506. https://doi.org/10.1016/j.physb.2023.415506

[44] Ezenwaka, L. N., Nwori, A. N., Ottih, I. E., Okereke, N. A., & Okoli, N. L. (2022). Investigation of the optical, structural and compositional properties of electrodeposited lead manganese sulfide (PbMnS) thin films for possible device applications. *Nanoarchitectonics*, *3*(1), 18-32. https://doi.org/10.37256/nat.3120221226

[45] Chloob, M. K., & Hussain, S. A. (2020). Study the Structural and Optical Properties Pure Copper Sulfide (CuS) Films Prepared by Pulsed Laser Deposition (PLD). Journal of Physics: Conference Series, 1591, 012014. DOI 10.1088/1742-6596/1591/1/012014